Eur Biophys J (2012) 41:491–503
DOI 10.1007/s00249-012-0804-x

ORIGINAL PAPER

EBSA
Biophysics in Europe

Role of t-tubules in the control of trans-sarcolemmal ion flux and intracellular Ca^{2+} in a model of the rat cardiac ventricular myocyte

M. Pásek · J. Šimurda · C. H. Orchard

Received: 20 January 2012 / Revised: 9 March 2012 / Accepted: 13 March 2012 / Published online: 1 April 2012

Abstract The t-tubules of mammalian ventricular myocytes are invaginations of the surface membrane that form a complex network within the cell, with restricted diffusion to the bulk extracellular space. The trans-sarcolemmal flux of many ions, including Ca^{2+}, occurs predominantly across the t-tubule membrane and thus into and out of this restricted diffusion space. It seems possible, therefore, that ion concentration changes may occur in the t-tubule lumen, which would alter ion flux across the t-tubule membrane. We have used a computer model of the ventricular myocyte, incorporating a t-tubule compartment and experimentally determined values for diffusion between the t-tubule lumen and bulk extracellular space, and ion fluxes across the t-tubule membrane, to investigate this possibility. The results show that influx and efflux of different ion species across the t-tubule membrane are similar, but not equal. Changes of ion concentration can therefore occur close to the t-tubular membrane, thereby altering trans-sarcolemmal ion flux and thus cell function, although such changes are reduced by diffusion to the bulk extracellular space. Slowing diffusion results in larger changes in luminal ion concentrations. These results provide a deeper understanding of the role of the t-tubules in normal cell function, and are a basis for understanding the changes that occur in heart failure as a result of changes in t-tubule structure and ion fluxes.

Keywords t-Tubules · Rat · Cardiac myocyte · Computer model · Calcium

Electronic supplementary material The online version of this article (doi:10.1007/s00249-012-0804-x) contains supplementary material, which is available to authorized users.

M. Pásek
Institute of Thermomechanics—Branch Brno,
Academy of Sciences of the Czech Republic,
Technická 2, 616 69 Brno, Czech Republic

M. Pásek (✉) · J. Šimurda
Department of Physiology, Faculty of Medicine,
Masaryk University, Kamenice 5,
625 00 Brno, Czech Republic
e-mail: mpasek@med.muni.cz

C. H. Orchard
School of Physiology and Pharmacology,
University of Bristol, Bristol BS8 1TD, UK

Introduction

The transverse (t-) tubules of mammalian cardiac ventricular myocytes are invaginations of the surface membrane that occur predominantly at the Z-line and form a complex network containing transverse and longitudinal elements. Recent work has provided structural and functional evidence that many of the proteins that underlie excitation–contraction coupling in these cells are located mainly at the t-tubules; thus most Ca^{2+} influx via L-type Ca^{2+} channels (LTCC), and subsequent release of Ca^{2+} from adjacent sarcoplasmic reticulum (SR) via ryanodine receptors (RyR's), and Ca^{2+} extrusion from the cell via Na^{+}–Ca^{2+} exchange and sarcolemmal Ca^{2+} ATPase, occur at the t-tubules (reviewed by Orchard et al. 2009; Chase and Orchard 2011). These ion fluxes occur into and out of a space—the t-tubule lumen—which has restricted diffusional access to the bulk extracellular space, a condition that will be exacerbated in the intact tissue in which diffusion will be restricted further by the limited volume of the inter-cellular clefts.

Thus it seems likely that ion fluxes occurring across the t-tubule membrane will alter the concentration of ions

within the t-tubule lumen which will, in turn, affect the membrane currents, thereby providing a negative feedback mechanism. Currents flowing across the t-tubule membrane may therefore be modulated physiologically by changes in extracellular (luminal) ion concentrations, as well as by ion concentrations at the cytoplasmic face of the channel, as described elsewhere (Eisner et al. 1998).

In addition, however, membrane currents at the t-tubules seem to be regulated differently from those at the surface membrane. For example, basal and stimulated protein kinase A (PKA) activity has a greater effect on L-type Ca^{2+} current (I_{Ca}) at the t-tubules than at the surface membrane (Brette et al. 2004a; Chase et al. 2010). More importantly for this study, regulation of I_{Ca} by Ca^{2+} at the cytoplasmic face of the LTCC seems to be different at the t-tubule and surface membranes, with inactivation of I_{Ca} being faster in the t-tubules than at the surface membrane (Brette et al. 2004b). This more rapid inactivation seems to be because of greater sensitivity of inactivation to Ca^{2+} released from the SR rather than to depletion of Ca^{2+} in the t-tubule lumen (because the time course of Ba^{2+} currents, which are larger than Ca^{2+} currents, is the same at the t-tubule and surface membranes (Brette et al. 2004b)). This faster inactivation would be predicted to have important consequences, including minimising Ca^{2+} depletion in the t-tubules without decreasing SR Ca^{2+} release, because the trigger for Ca^{2+} release is predominantly early Ca^{2+} influx via I_{Ca} (Fabiato 1985; Beuckelmann and Wier 1988). However such predictions are not currently amenable to experimental investigation.

In this study we have, therefore, used a computer model of the rat cardiac ventricular myocyte, including a t-tubular compartment and the most recent available experimental data, to investigate the effect of this differential modulation of I_{Ca} at the t-tubular and surface membranes on Ca^{2+} handling, and the role of the t-tubules in modulating Ca^{2+} fluxes.

Methods

The model used in this study is based on that described elsewhere (Pásek et al. 2006), which has been modified to incorporate separate t-tubular and surface membrane dyads with different Ca^{2+}-dependent regulation of I_{Ca} at the two sites (Brette et al. 2004b; see "Introduction"), and ion gradients in the sub-sarcolemmal space and t-tubule lumen. This has been achieved by:

1. incorporating separate dyadic spaces adjacent to the t-tubular and surface membranes;
2. incorporating junctional SR compartments adjacent to the t-tubular and surface dyadic spaces (JSR_t and JSR_s);
3. incorporating sub-sarcolemmal spaces adjacent to the t-tubular and surface membranes; and
4. partitioning the space within the t-tubule lumen into nine concentric cylindrical segments.

In addition, the model was modified:

1. to enable diffusion of exogenous Ca^{2+} buffers between a patch pipette and intracellular spaces;
2. to include Ca^{2+} buffering in the t-tubules;
3. to increase the t-tubular fraction of sarcolemmal Ca^{2+} ATPase to 95 % (Chase and Orchard 2011); and
4. to improve description of SR Ca^{2+} pump and ryanodine receptor function.

These modifications are described in greater detail in the Online Resource; the model is illustrated in Fig. 1.

The model was implemented in MATLAB v.7.2 (MathWorks, Natick, MA, USA). Numerical computation of the system of 97 nonlinear differential equations was performed by use of the solver for stiff system ODE-15s. The model equations were simultaneously solved using a time-step adjusted to keep the estimated relative error of inner variables below a threshold value of 10^{-6}. The stability of the model was tested by running the model for 1 h periods of equivalent cell lifetime at different stimulation frequencies. The basic units in which the equations were solved were mV for membrane potential, mA for membrane currents, mM for ion concentrations, s for time, and ml for volumes.

Results

Stability of the model

To ensure that the model is stable for prolonged periods, and changes appropriately and reversibly in response to intervention, it was initially run for periods of several hours, as described in the "Methods" section. This is necessary to show that the model is valid, and appropriate for time-dependent measurements. Figure 2 shows the values for cytoplasmic, end-diastolic $[Ca]^{2+}$ (top), $[Na]^{+}$ (middle), and $[K]^{+}$ (bottom) during a 5-h run in which the model cell was at rest, and stimulated at 1, 3, and 5 Hz, as indicated above the traces, showing the stability of the model with time, the changes that occur during stimulation at different frequencies, and the reversibility of these changes.

Ion concentration changes in the t-tubule lumen during activity

Changes in ion concentrations within the t-tubule lumen during activity may be important in modulating membrane currents across the t-tubule membrane, and hence intracellular ion concentrations (see "Introduction"); however they have not yet proved tractable to experimental measurement.

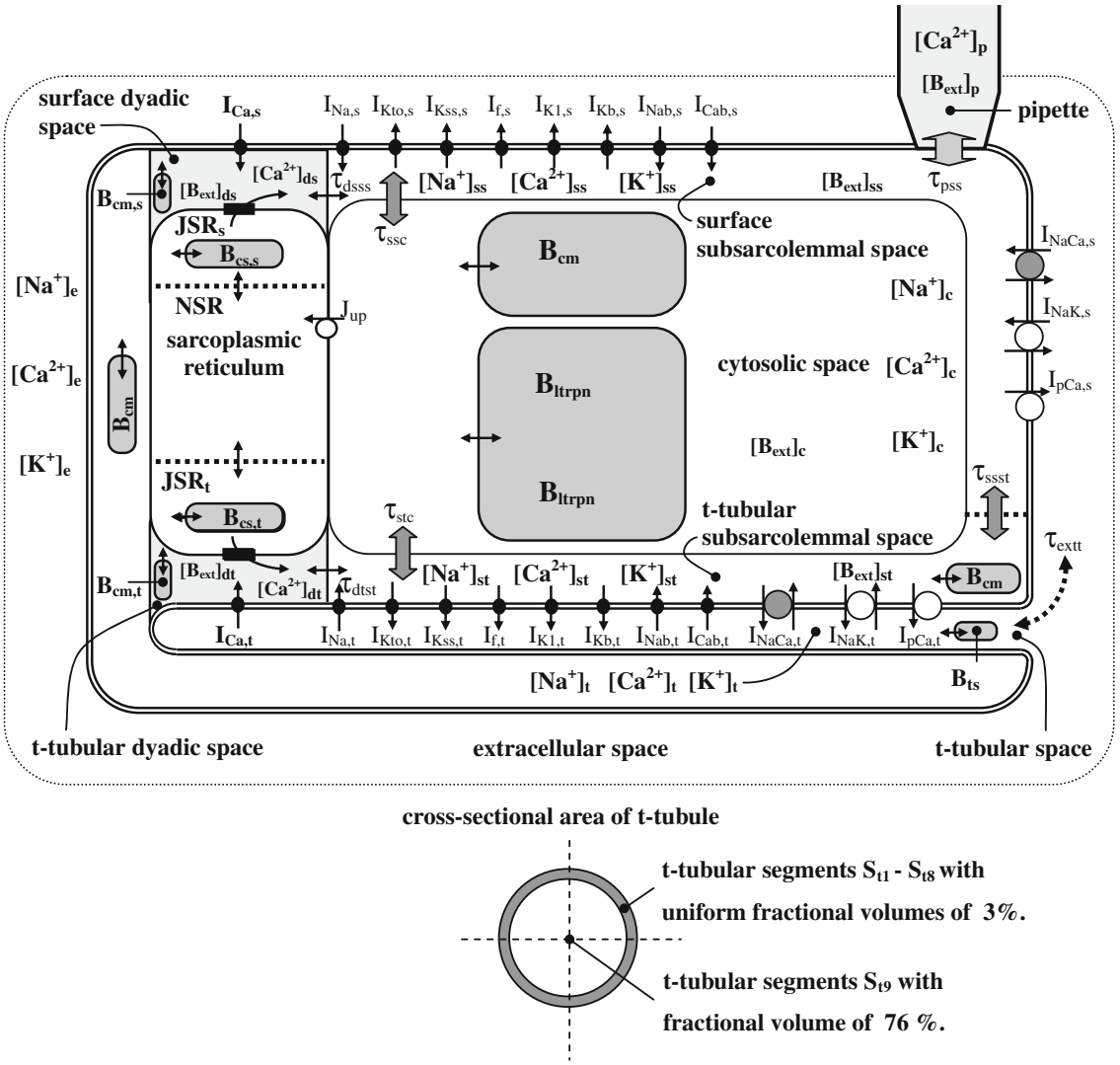

Fig. 1 Schematic diagram of the rat ventricular cell model used in this study. Description of the electrical activity of surface (*s*) and t-tubular (*t*) membranes entails formulation of the following ion currents: fast sodium current (I_{Na}), L-type calcium current (I_{Ca}), transient outward potassium current (I_{Kto}), steady-state outward potassium current (I_{Kss}), inward rectifying potassium current (I_{K1}), hyperpolarization-activated current (I_f), background currents (I_{Kb}, I_{Nab}, I_{Cab}), sodium–calcium exchange current (I_{NaCa}), sodium–potassium pump current (I_{NaK}), and calcium pump current (I_{pCa}). The intracellular space contains the cytosolic space (c), surface and t-tubular subsarcolemmal subspaces (ss, st), surface and t-tubular dyadic spaces (d*t*, d*s*), network and junctional compartments of the sarcoplasmic reticulum (NSR, JSR_s, JSR_t), endogenous Ca^{2+} buffers (calmodulin (B_{cm}), troponin (B_{htrpn}, B_{ltrpn}), calsequestrin (B_{cs})), and exogenous Ca^{2+} buffer (e.g. BAPTA or EGTA; B_{ext}). The t-tubular space is partitioned into nine concentric segments, S_{t1}–S_{t9}; a schematic representation of this partitioning is shown under the diagram and the details are given in the Online Resource. B_{ts} denotes the non-specific Ca^{2+} buffer associated with the luminal part of the t-tubular membrane. J_{up} represents Ca^{2+} flow via the SR Ca^{2+} pump and the small filled rectangles in JSR membrane ryanodine receptors. The small *bi-directional arrows* denote Ca^{2+} diffusion. Ion diffusion between the t-tubular and extracellular space is represented by the *dashed arrow*. Variables relating to the cellular membrane were set according to the results published by Pásek et al. (2008) (11); the fractional area of the t-tubular membrane was reduced to 49 % and the specific capacitances of the t-tubular and surface membranes were set to 1.275 and 0.714 μF/cm^2, respectively. This adjustment is consistent with the commonly used value of the total membrane specific capacitance of 1 μF/cm^2

We have, therefore, used the model to investigate such changes.

Figure 3a, b show $[Ca^{2+}]$ and $[K^+]$ in the 1st (adjacent to the cell membrane) 3rd, 5th, 7th, and 9th (central) segments of the t-tubule lumen ($[Ca^{2+}]_t$ and $[K^+]_t$) in the model during action potentials. Figure 3a shows changes during the first action potential from rest showing rapid initial Ca^{2+} depletion, associated with I_{Ca}, followed by a rise of $[Ca^{2+}]_t$ to a level slightly higher than $[Ca^{2+}]$ in the bulk extracellular space (see the section "Ca^{2+} and K^+ cycling between t-tubular and peripheral membrane" and the "Discussion"). In contrast, for $[K^+]_t$ an initial transient increase caused by

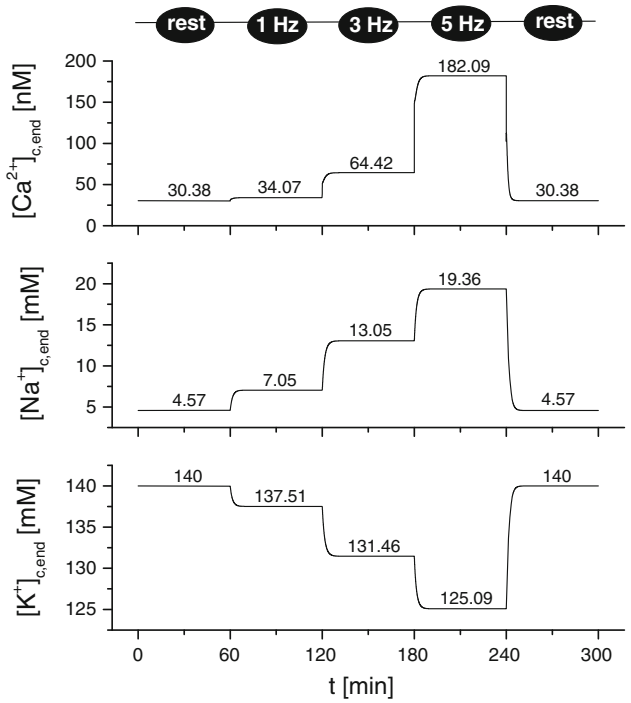

Fig. 2 Stability of the model, showing cytoplasmic, end-diastolic $[Ca^{2+}]$ (*top*), $[Na^+]$ (*middle*), and $[K^+]$ (*bottom*) during a 5 h run during which the model cell was at rest, and stimulated at 1, 3 and 5 Hz, as indicated above the traces

I_{Kto}, the dominant K^+ current in rat ventricular myocytes, is observed, followed by a slow decrease; the re-uptake of K^+ into the myocyte via the Na^+–K^+ ATPase is relatively slow so that the decrease of $[K^+]_t$ depends mainly on the rate of diffusion of K^+ to the extracellular space. Figure 3b shows equivalent data at steady-state during 5-Hz stimulation. The steady levels of $[K^+]_t$ in all segments are slightly lower than extracellular $[K^+]$.

Figure 3c shows the changes of $[Ca^{2+}]$ and $[K^+]$ in the first t-tubular segment ($\Delta[Ca^{2+}]_{t1}$, $\Delta[K^+]_{t1}$) during an AP elicited from rest and during 1, 3, and 5 Hz steady-state stimulation. An increase in stimulation frequency results in a smaller initial decrease of $[Ca^{2+}]_{t1}$ and an increase of the mean value of $[Ca^{2+}]_{t1}$ ($\Delta[Ca^{2+}]_{t1,mean}$, shown by the dashed line, related to extracellular level). The initial increase of $\Delta[K^+]_{t1}$ declines with increasing stimulation frequency and the mean value of $[K^+]_{t1}$ ($\Delta[K^+]_{t1,mean}$) remains close to the extracellular level.

The results shown in Fig. 3 can be explained in terms of an expression (Eq. 1) derived from the model equations, which in its general form is valid for all ion species but is specified here for Ca^{2+} for clarity.

$$\Delta\left[Ca^{2+}\right]_{t1,mean} = \left[Ca^{2+}\right]_{t1,mean} - \left[Ca^{2+}\right]_e = K\left(\tau_{Ca,extt} \cdot f \cdot n_{Ca,net,t}\right) \quad (1)$$

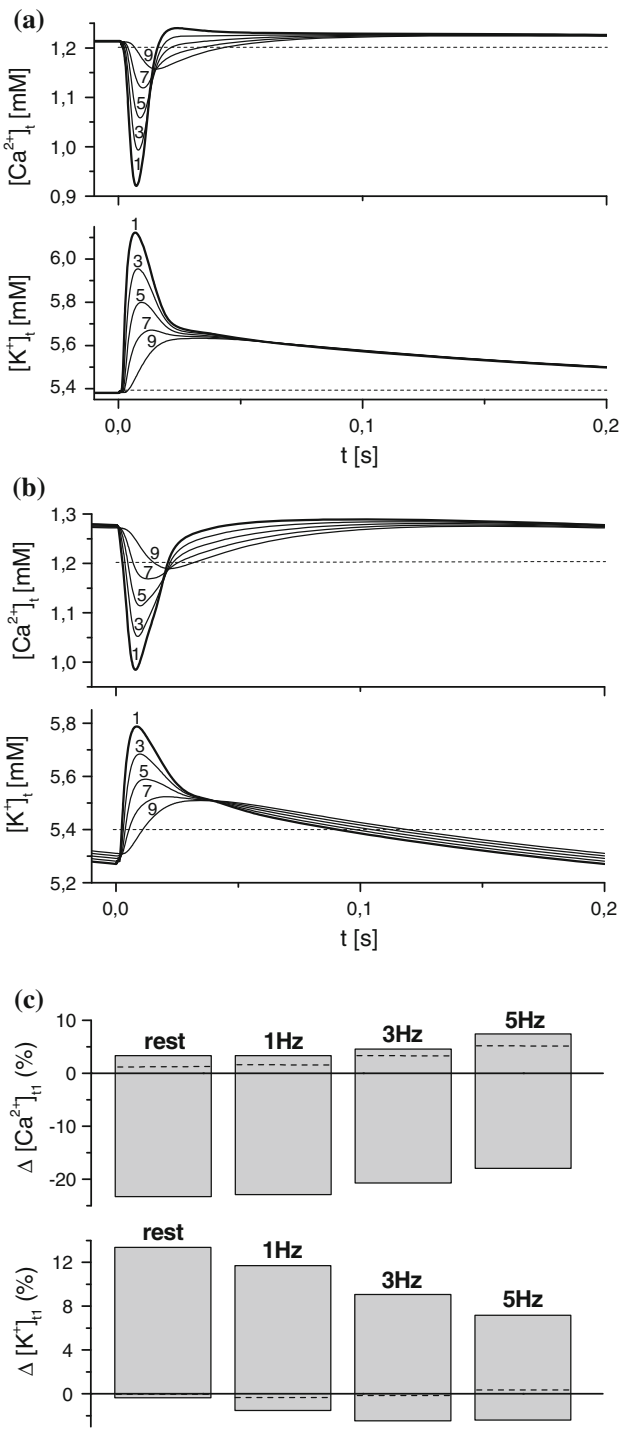

Fig. 3 *Top* $[Ca^{2+}]$ and $[K^+]$ in t-tubular segments 1, 3, 5, 7, and 9 during an action potential elicited from rest (**a**) and during 5-Hz steady-state stimulation (**b**). *Lower panel* Relative changes of $[Ca^{2+}]_t$ ($\Delta[Ca^{2+}]_t$) and $[K^+]_t$ ($\Delta[K^+]_t$) during APs elicited from rest and during 1, 3, and 5-Hz steady-state stimulation. The changes are related to extracellular concentrations $[Ca^{2+}]_e = 1.2$ mM and $[K^+]_e = 5.4$ mM. The *dotted lines* within the *bars* indicate the resting (*rest*) or mean tubular concentrations (1, 3, and 5 Hz)

In the steady state, the deviation of mean $[Ca^{2+}]$ in the first t-tubular segment from $[Ca^{2+}]_e$ is directly proportional to three quantities:

1. the time constant for Ca^{2+} diffusion from the external space to the t-tubule lumen ($\tau_{Ca,extt}$);
2. the stimulation frequency (f); and
3. the net amount of Ca^{2+} transferred across the t-tubular membrane during a stimulation period ($n_{Ca,net,t}$).

K (in l^{-3}) is a constant. $n_{Ca,net,t}$ is represented by the integral of net Ca^{2+} flow ($J_{Ca,net,t}$).

$$n_{Ca,net,t} = \int_T J_{Ca,net,t}\,dt = \frac{1}{2F}\int_T (I_{Ca,t} - 2I_{NaCa,t} + I_{Cab,t} + I_{pCa,t})dt. \quad (2)$$

Although the relationship between $\Delta[Ca^{2+}]_{t1,mean}$ and stimulation rate is nearly linear, the frequency dependence of $\Delta[K^+]_{t1,mean}$ deviates markedly from direct proportionality, because of the strong frequency dependence of $n_{K,net,t}$ (Fig. 8 and "Discussion").

The resting state can be regarded as a limit for $T \to \infty$, the Eq. 1 for resting value $[Ca^{2+}]_{t,rest}$ gives:

$$[Ca^{2+}]_{t1,rest} - [Ca^{2+}]_e = K(\tau_{Ca,extt} \cdot J_{Ca,net,t}), \quad (3)$$

where $J_{Ca,net,t}$ is the net flux of Ca^{2+} across the t-tubular membrane at rest. Equations 1 and 3 also show that the deviation of $[Ca^{2+}]_{t1,mean}$ from $[Ca^{2+}]_e$ results primarily from the unequal distribution of ion currents between the t-tubular and surface membranes and the consequent cycling of ions between these membranes (see the section "Ca^{2+} and K^+ cycling between t-tubular and peripheral membrane"). If the distribution were equal, $n_{Ca,net,s}$ and $n_{Ca,net,t}$ would be zero for each membrane and $[Ca^{2+}]_{t1,mean}$ would be equal to $[Ca^{2+}]_e$. The same considerations are valid for K^+ and Na^+.

To investigate further the extent to which ion concentrations in the t-tubule lumen are determined by diffusion between the lumen and the bulk extracellular space, as opposed to trans-sarcolemmal ion flux, the effect of inhibiting diffusion (τ_{extt} set to 1,000 s) on luminal ion concentrations was determined. Figure 4 shows that inhibiting diffusion led to a marked increase in tubular Na^+ and Ca^{2+} concentrations over several minutes, as a result of net efflux of these ions across the t-tubule membrane (for Ca^{2+}, mainly through I_{pCa}), which normally has little effect on tubular concentration because of the corresponding flux to the bulk extracellular space, which seems to stabilise luminal concentrations. However, K^+ is only slightly affected because of an increase of $I_{K1,t}$ as $[K^+]_t$ decreases.

Effect of changes of luminal ion concentrations on membrane currents and the Ca^{2+} transient

The results described above suggest that activity-induced ion transport across the t-tubular membrane alters ion concentrations in the t-tubular lumen. We investigated, therefore, the extent to which these changes modulate t-tubular membrane currents during an action potential (AP) and a voltage clamp (VC) pulse.

Figure 5a shows the temporal relationship between the changes in $[Ca^{2+}]_{t,1}$ described above and the associated Ca^{2+} currents during an action potential (dotted lines). To investigate whether the change of luminal $[Ca^{2+}]$ modulates Ca^{2+} flux across the t-tubule membrane, the experiment was repeated while the $[Ca^{2+}]$ in the t-tubule lumen was held constant at the concentration in the bulk extracellular space (solid lines). The differences between Ca^{2+}

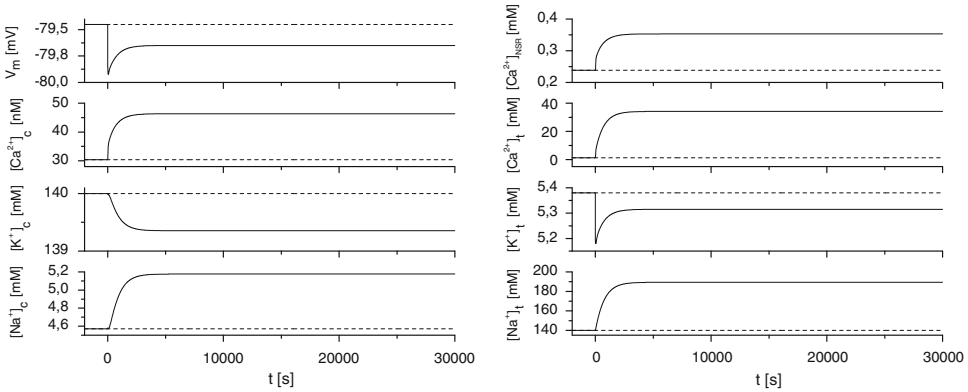

Fig. 4 Effect of inhibition of ion diffusion between the t-tubule lumen and bulk extracellular space on resting membrane potential (V_m), tubular ion concentrations ($[Ca^{2+}]_t$, $[K^+]_t$ and $[Na^+]_t$) and intracellular ion concentrations ($[Ca^{2+}]_{NSR}$, $[Ca^{2+}]_c$, $[K^+]_c$, $[Na^+]_c$). Inhibition of diffusion was achieved by increasing τ_{extt} from 0.22 s (*dashed line*) to 1,000 s (*solid line*) at time $t = 0$ s

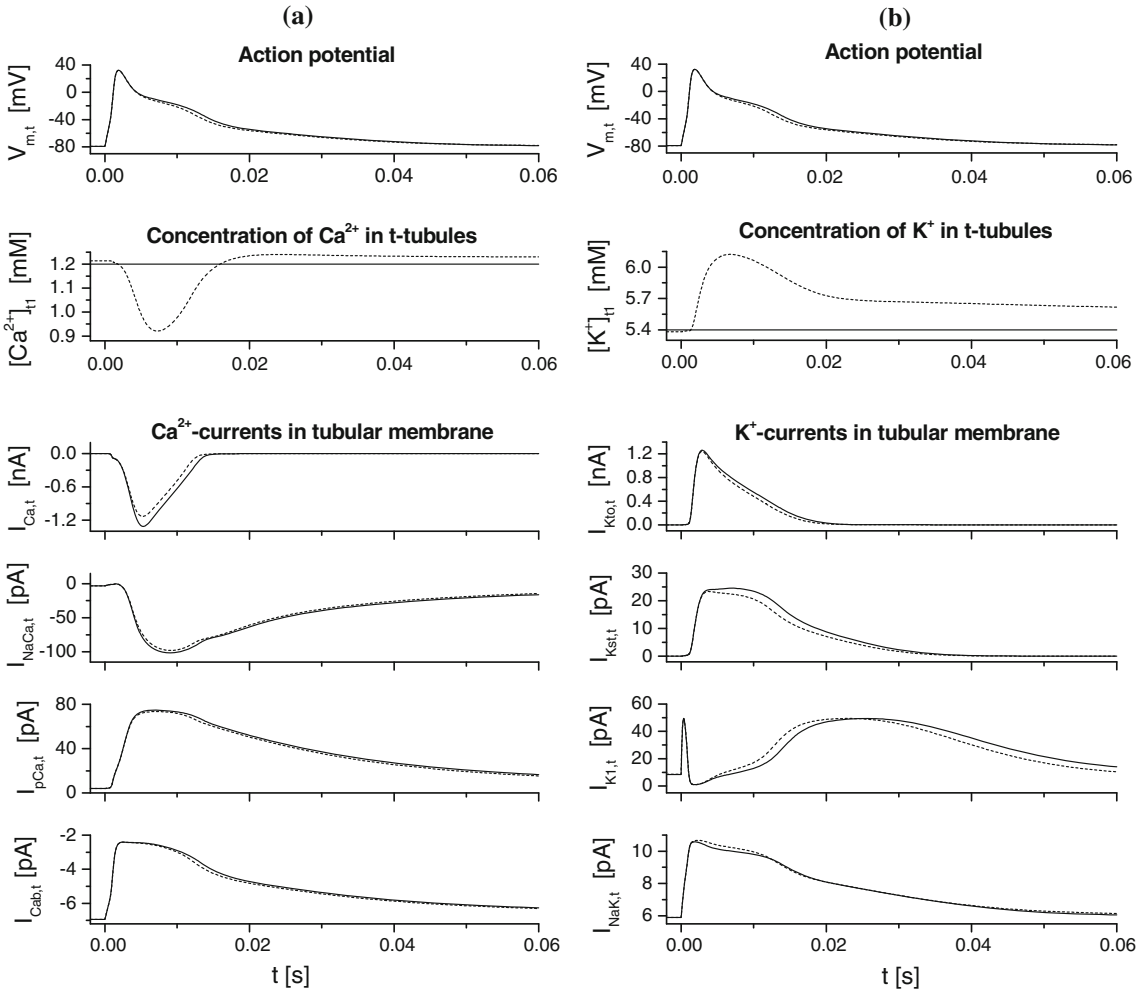

Fig. 5 Effect of ion concentration changes in the first t-tubular segment on t-tubular ionic currents during an action potential elicited from resting potential (−79.45 mV). **a** Effect of changes of $[Ca^{2+}]_{t,1}$ on $I_{Ca,t}$, $I_{NaCa,t}$, $I_{pCa,t}$, and $I_{Cab,t}$. **b** Effect of changes of $[K^+]_{t,1}$ on $I_{Kto,t}$, $I_{Kst,t}$, $I_{K1,t}$, and I_{NaK}. *Dotted lines*, model in which ion concentrations within the t-tubule lumen were allowed to change; *solid lines*, model with tubular ion concentration fixed at bulk extracellular levels

currents in each condition indicate that the decrease of luminal $[Ca^{2+}]$ has a small but visible effect on Ca^{2+} fluxes across the t-tubule membrane. Figure 5b shows corresponding data for $[K^+]$, showing that the $I_{Kto,t}$-induced rise of $[K^+]_{t,1}$ leads to a decrease of $I_{Kto,t}$, $I_{Kst,t}$ and an increase in $I_{K1,t}$ followed by a decrease during the late phase of the AP.

Figure 6 shows corresponding data during a 100-ms VC pulse from resting potential to 0 mV. Although Ca^{2+} depletion affects Ca^{2+} currents only slightly, there is marked accumulation of tubular K^+ (from 5.4 to ~6.3 mM) during prolonged depolarization which resulted in a decrease of $I_{Kst,t}$, an increase of $I_{NaK,t}$, and development of a marked $I_{K1,t}$ tail current because of the shift of the reversal potential for K^+ to more positive values.

To investigate whether these changes in membrane currents alter the Ca^{2+} transient we monitored the Ca^{2+} transient in the model during stimulation at 5 Hz, the frequency that corresponds to the normal heart rate in rat. Figure 7 shows that the decrease in luminal Ca^{2+} concentration resulted in a decrease in the amplitude of the Ca^{2+} transient (dotted line) compared with the situation in which luminal $[Ca^{2+}]$ was fixed at bulk extracellular concentration (solid line). Two main factors were responsible for the altered Ca^{2+} transient in the model. The first was the decrease in the amount of Ca^{2+} entering the t-tubular dyadic space via $I_{Ca,t}$ ($n_{Ca,t}$, the Ca^{2+} "trigger" for SR Ca^{2+} release) as a result of the decrease in $[Ca^{2+}]_{t,1}$. The second was the associated decrease of SR Ca^{2+} load ($[Ca^{2+}]_{NSR,end}$). The table in Fig. 7 shows the percentage decrease (compared with when $[Ca^{2+}]_t$ was fixed at $[Ca^{2+}]_e$) in $n_{Ca,t}$ and $[Ca^{2+}]_{NSR,end}$, and the resulting decrease in the peak of the cytosolic Ca^{2+} transient $[Ca^{2+}]_{c,peak}$, that occurs as a result of the decrease in $[Ca^{2+}]_{t,1}$.

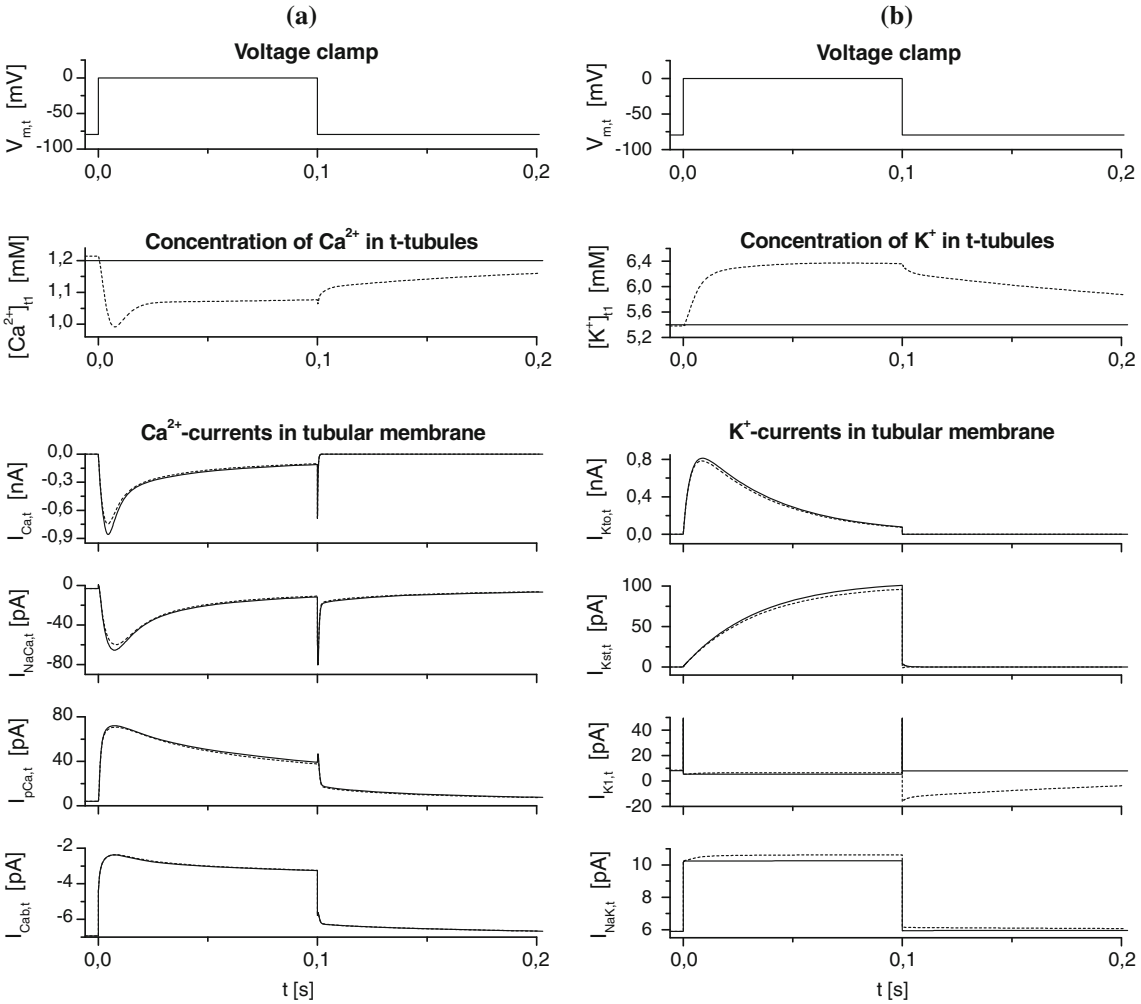

Fig. 6 Effect of ion concentration changes in the first t-tubular segment on t-tubular ionic currents during and after termination of a 0.1-s voltage-clamp pulse from resting potential (−79.45 mV) to 0 mV. **a** Effect of changes of $[Ca^{2+}]_{t,1}$ on $I_{Ca,t}$, $I_{NaCa,t}$, $I_{pCa,t}$, and $I_{Cab,t}$. **b** Effect of changes of $[K^+]_{t,1}$ on $I_{Kto,t}$, $I_{Kst,t}$, $I_{K1,t}$, and I_{NaK}. *Dotted lines*, model in which ion concentrations within the t-tubule lumen were allowed to change; *solid lines*, model with tubular ion concentration fixed at bulk extracellular levels

Ca^{2+} and K^+ cycling between t-tubular and peripheral membrane

The distribution of ion transporters in the model (Table 1 in the Online Resource) and the data shown above (Fig. 3) suggest that Ca^{2+} and K^+ influx and efflux are not exactly matched across the t-tubule and surface membranes. However, if the model is to be stable (Fig. 2), the time-averaged influx of each ion must equal its time averaged efflux from the cell. Thus, if influx and efflux are unequal at the t-tubular membrane and the surface membrane, this suggests that the mismatch at one site must be compensated at the other, leading to the possibility of ion cycling between the t-tubule and surface membranes. To test this idea, we investigated influx and efflux of Ca^{2+} and K^+ across each membrane. Figure 8 shows the integrals of the ion fluxes via each pathway during a single cycle at steady state, representing ion transfer across the surface (white bars) and t-tubular (black bars) membranes, showing that ion transfer by each pathway during a cycle is different across each membrane, and that the relative proportions change with stimulation frequency. Summing these fluxes shows net Ca^{2+} influx across the surface membrane ($n_{Ca,net,s}$), and the same amount of Ca^{2+} leaving the cell through the t-tubule membrane ($n_{Ca,net,t}$). This suggests a net movement of Ca^{2+} from the surface membrane to the t-tubule membrane, which maintains the steady state (Fig. 2). These net amounts, however, become smaller at increased stimulation rates. Conversely, for K^+ a net influx is observed at the t-tubules ($n_{K,net,t} < 0$) and net efflux across the surface membrane ($n_{K,net,s} > 0$), suggesting net movement of this ion in the direction opposite to that of

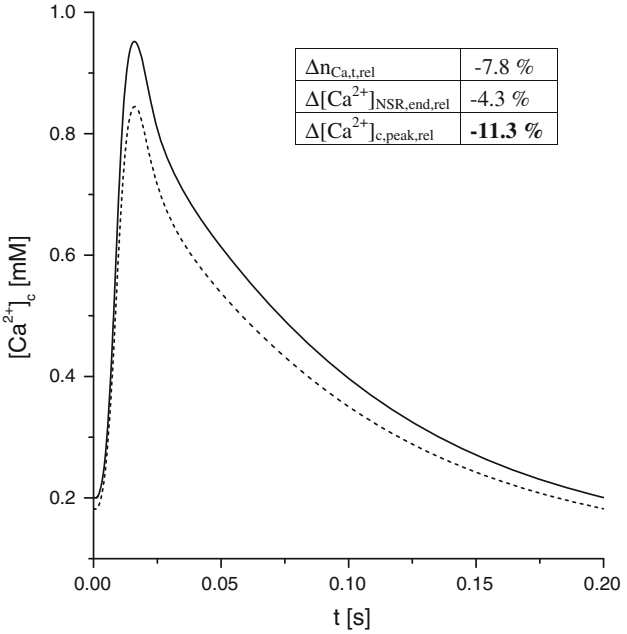

Fig. 7 Effect of ion concentration changes in t-tubules on the magnitude of the steady-state systolic Ca^{2+} transient during an action potential at a stimulation frequency of 5 Hz. The *solid* and *dotted lines* represent the Ca^{2+} transient in the model with tubular ion concentrations fixed at bulk extracellular levels and allowed to change, respectively. The values in the table show the relative changes in the amount Ca^{2+} entering the t-tubular dyadic space via $I_{Ca,t}$ during the cycle ($\Delta n_{Ca,t,rel}$), the changes in SR Ca^{2+} load at the end of the cycle ($\Delta[Ca^{2+}]_{NSR,end,rel}$), and changes in the peak value of the cytosolic Ca^{2+} transient ($\Delta[Ca^{2+}]_{c,peak,rel}$)

Ca^{2+}, although the net fluxes, like those of Ca^{2+}, became smaller as the stimulation frequency was increased. At 5 Hz, the direction of residual cycling is reversed.

Discussion

The t-tubules of mammalian cardiac ventricular myocytes form a restricted diffusion space into and out of which trans-sarcolemmal ion fluxes occur. Changes of ion concentrations within a restricted diffusion space between cells in cardiac tissue, and their functional sequelae, have been recognized for more than 30 years (Kline and Morad 1978; Baumgarten et al. 1977; Attwell et al. 1979), but more recent work, in isolated myocytes, has also provided evidence of changes of ion concentrations within t-tubules during activity (Clark et al. 2001; Swift et al. 2006). Our work provides a quantitative framework for understanding the role of the t-tubules in regulating ion homeostasis in ventricular myocytes in a way that is not currently tractable using experimental approaches, and shows the relationships between trans-sarcolemmal ion fluxes, diffusional ion exchange with the bulk extracellular space, and luminal ion concentrations.

The model

The model used in this study incorporates a number of key modifications necessary to reproduce recent experimental data (see "Methods" section). The main factors affecting $[Ca^{2+}]$ in the t-tubule lumen in the model are:

1. The distribution of ion transporters between the t-tubule and surface membranes. The distributions used in the model are based predominantly on those determined experimentally using acute detubulation of rat ventricular myocytes, as described elsewhere (Pásek et al. 2008). The main change was in the distribution of the sarcolemmal Ca^{2+} ATPase, which recent work (Chase and Orchard 2011) has shown to be located almost exclusively in the t-tubular membrane, so that its t-tubular fraction was set to 95 %. The importance of this distribution is illustrated in Fig. 9, which shows that the absence of Ca^{2+} ATPase from the t-tubular membrane reduces the cytosolic Ca^{2+} transient, as a result of a decrease of tubular $[Ca^{2+}]$.
2. The rate of diffusion of ions between the t-tubule lumen and the extracellular space. The rate used in the model is based on experimental data in which rapid changes of extracellular ion concentrations led to a biphasic change of resting membrane potential or membrane currents (Yao et al. 1997). The changes in resting membrane potential (Fig. 1 of Yao et al. 1997) are probably a result of simple diffusion of K^+ (Pásek et al. 2006); however, the more complex change in I_{Ca} (Fig. 6 of Yao et al. 1997) seems to involve other factors. Reconstruction of these experiments in the model (see the Online Resource) shows that buffering of Ca^{2+} in the t-tubular lumen may account for the changes observed.

Because changes of ion concentration are expected to be largest, and most important, close to the t-tubular membrane, because of trans-sarcolemmal ion fluxes, the model incorporates radial gradients within the t-tubules. To simulate such gradients the t-tubular lumen was partitioned into nine concentric cylindrical segments; the time constants controlling the rate of ion exchange between neighbouring segments were determined from $\tau_{Ca,extt}$ and the geometrical properties of the segments (see Online Resource). The simulations showed that, during activity, Ca^{2+} changes are larger close to the t-tubular membrane than in the centre of the lumen. Figure 9 shows that this reduces the size of the Ca^{2+} transient, compared with a single-compartment model, as a result of greater depletion of Ca^{2+} adjacent to the t-tubular membrane during activation of I_{Ca}. It is worth noting, however, that the model lacks longitudinal diffusion gradients within the t-tubules, which have a more complex structure than the

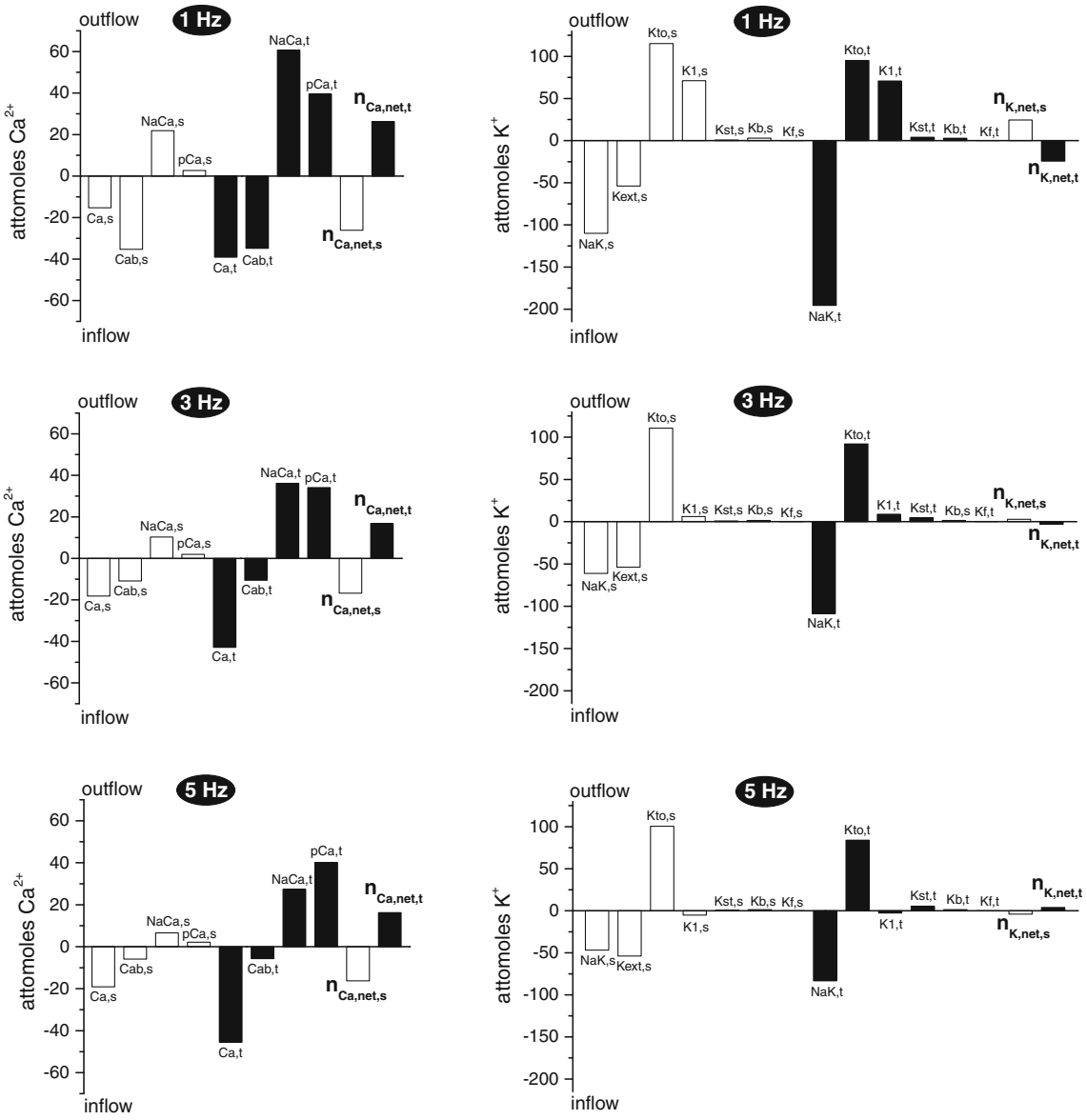

Fig. 8 Amount of Ca^{2+} (*left*) and K^+ (*right*) transferred by each ion flux pathway across the surface (*white bars*) and t-tubule (*black bars*) membranes during stimulation by steady-state cycling at frequencies of 1 Hz (*top*), 3 Hz (*middle*), and 5 Hz (*bottom*). Influx is shown downwards, efflux upwards. Net ion flux across each membrane is shown in the *right bars* in each panel

representation in the model, and ion flux pathways may be heterogeneously distributed; in a previous modelling study we suggested that concentration changes deep within the t-tubules are greater than near the t-tubule mouth, and that the irregular spatial distribution of [Ca^{2+}] within the t-tubules that results from irregular clustered distribution of Ca^{2+} channels dissipates within 150 ms of initiation of I_{Ca}, because of diffusion and Ca^{2+} buffering (Šimurda et al. 2004). It has also been suggested that changes in t-tubule dimensions during mechanical activity accelerate ion exchange by "assisted convection" (Kohl et al. 2003); this suggestion is supported by the observation that cellular strain reduces the length and volume of the t-tubules, which would be expected to increase fluid exchange between the t-tubule lumen and extracellular space (McNary et al. 2011). Such exchange would, therefore, increase with activity, thereby reducing changes in luminal ion concentrations at higher frequencies.

However the model used in this study is based as far as possible on experimental data and is, importantly, stable for long periods, enabling time-dependent studies to be performed and, despite limitations, effectively reproduces experimentally observed behaviour in intact and detubulated myocytes.

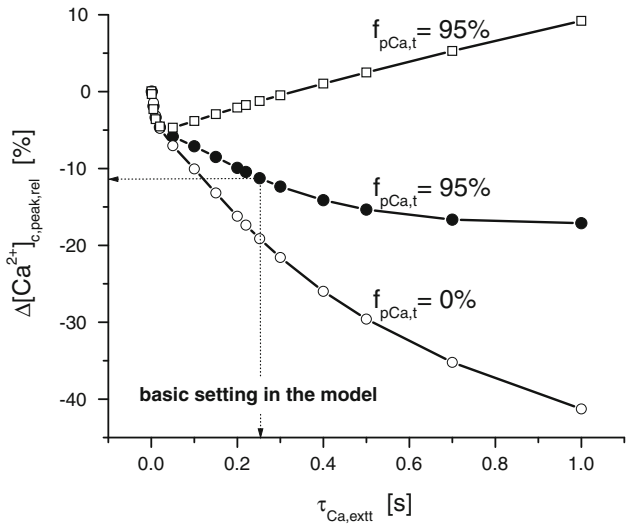

Fig. 9 The relationship between the peak of the systolic Ca^{2+} transient, $[Ca^{2+}]_{c,peak}$ ($\Delta[Ca^{2+}]_{c,peak,rel}$), and the time constant for Ca^{2+} exchange between the extracellular space and the t-tubule lumen ($\tau_{Ca,extt}$) at 5 Hz stimulation. *Black circles*, *white circles*, and *white squares* show, respectively, results from the basic model, those from the model after reducing f_{pCa} from 95 to 0 %, and those from the model after reformulating the t-tubular space as a single compartment. $\Delta[Ca^{2+}]_{c,peak}$ is expressed relative to steady-state $[Ca^{2+}]_{c,peak}$ (0.95 μM) at 5 Hz stimulation in the model with tubular ion concentrations fixed at extracellular levels and $f_{pCa} = 95$ %

The relationship between trans-membrane ion flux, rate of diffusion, and tubular ion concentration

Equation 1, which describes a steady state, can be used to analyse the relationship between mean ion concentrations in t-tubular subsarcolemmal space (dotted lines in Fig. 3), trans-membrane ion flux ($n_{Ca,net,t}$ in Fig. 8), frequency, and $\tau_{Ca,extt}$. This shows that deviation of mean tubular concentration of each ion from the bulk extracellular concentration (Fig. 3) results from net ion flux across the t-tubule membrane: inserting $n_{Ca,net,t} = 0$ into Eq. 1 gives $[Ca^{2+}]_{t,mean} = [Ca^{2+}]_e$. At steady state, $-n_{Ca,net,s} = n_{Ca,net,t} = n_{Ca,net,t-e}$, where $n_{Ca,net,t-e}$ is the amount of Ca^{2+} diffusing from the t-tubule lumen to the bulk extracellular space during a cycle. Complete inhibition of diffusion would eventually result in zero net ion flux across the t-tubular and surface membrane ($n_{Ca,net,t} = n_{Ca,net,s} = n_{Ca,net,t-e} = 0$) and each membrane subsystem would equilibrate separately. Under conditions of slowed diffusion (prolonged $\tau_{Ca,extt}$) according to Eq. 1, the system can reach equilibration (at unaltered frequency) in two ways:

1. as a result of an increase in the difference between $[Ca^{2+}]_{t,mean}$ and $[Ca^{2+}]_e$, as shown in Fig. 4; and
2. as a result of a decrease of $n_{Ca,net,t}$.

Although different in magnitude, the same considerations apply to other ions.

The role of the t-tubules in Ca^{2+} handling

Experimental work has shown that most trans-sarcolemmal Ca^{2+} flux occurs across the t-tubule membrane, and thus into and out of the restricted diffusion space formed by the t-tubule lumen. Thus it seemed possible that, unless influx was equal to efflux, changes in luminal Ca^{2+} concentration could occur, which would alter the magnitude of currents flowing across the t-tubule membrane, thereby modulating Ca^{2+} cycling and the inotropic state of the cell.

This work suggests that rate-dependent beat-to-beat changes of $[Ca^{2+}]$ occur within the t-tubule lumen, and are particularly marked close to the t-tubule membrane. The changes within a beat can be ascribed to rapid Ca^{2+} influx via I_{Ca}, followed by slower Ca extrusion via Na^+–Ca^{2+} exchange and the sarcolemmal Ca^{2+} ATPase, which occurs predominantly into the t-tubule lumen. The changes that occur over a longer time scale (for example after a change of the frequency of stimulation) are the result of altered net efflux into the t-tubule lumen balanced against diffusion to the extracellular space. Thus anything that changes either of these conditions will alter luminal Ca^{2+} and, in principle, the Ca^{2+} balance of the cell.

Slowing diffusion increases luminal Ca^{2+} concentration (Fig. 4), thus altering cellular Ca^{2+} homeostasis. This suggests a mismatch between Ca^{2+} influx and efflux across the t-tubule membrane and, hence—because cellular Ca^{2+} balance is maintained—across the surface membrane. Analysis of ion fluxes across each membrane revealed net Ca^{2+} influx across the surface membrane and net efflux across the t-tubule membrane into the t-tubule lumen.

Several mechanisms will affect Ca^{2+} efflux and influx at the t-tubule membrane, in particular:

1. distribution of protein function, as outlined above;
2. more marked CDI at the t-tubule membrane results in a smaller Ca^{2+} influx than would otherwise occur, although this will be offset by localised stimulation of I_{Ca} by basal PKA activity, which will increase Ca^{2+} influx;
3. localised stimulation of I_{NaCa} by basal PKA activity at the t-tubules has also been proposed (Chase and Orchard 2011), and t-tubular Na^+–Ca^{2+} exchangers seem to have preferential access to Ca^{2+} released from the SR (Trafford et al. 1995), both of which increase Ca^{2+} efflux and contribute to the observed net Ca^{2+} efflux;
4. negative feedback regulation, whereby a decrease of luminal $[Ca^{2+}]$ will reduce I_{Ca} and increase Ca^{2+} extrusion.

Thus the regulation of Ca^{2+} fluxes by Ca^{2+}, which has been proposed to underlie autoregulation of cell Ca^{2+}

(Eisner et al. 1998) and has been suggested to occur predominantly at the t-tubules (Orchard et al. 2009) may contribute to Ca^{2+} homeostasis in the t-tubule lumen.

Such regulation is likely to have implications during pathological conditions in which t-tubule structure (and hence diffusion times), PKA activity (and hence relative ion fluxes), and protein expression (and possibly distribution) are altered. Under these conditions it is unclear whether the changes of luminal ion concentration reported in this study would be exacerbated, unchanged, or reduced, with the corresponding functional sequelae. However the relatively small changes in luminal $[Ca^{2+}]$ may be important because the t-tubules therefore synchronise Ca^{2+} release and uptake without ion depletion, which may limit contraction, or accumulation, which may be arrhythmogenic.

The role of the t-tubules in Na^+ and K^+ handling

Although explored in less detail than Ca^{2+} in this study, it seems that t-tubules are also involved in regulation of Na^+ and K^+.

Figure 3 shows activity-dependent changes in K^+ that are similar to, although opposite in direction to, those observed for Ca^{2+}. Figure 4 shows that inhibition of diffusion results in a marked increase in $[Na^+]_t$ (as well as $[Ca^{2+}]_t$). However, $[K^+]_t$ decreases because of a small imbalance between $I_{NaK,t}$ and outward K^+-currents in the t-tubular membrane. At physiological stimulation frequencies, net K^+ flux seems to be smaller than net Ca^{2+} flux (Fig. 8), implying that K^+ influx more closely equals K^+ efflux across the t-tubular and surface membranes.

Early work using K^+-selective microelectrodes showed rate-dependent accumulation of K^+ in the extracellular space of frog ventricular muscle (Kline and Morad 1978), which lacks t-tubules, because of net K^+ efflux during a series of action potentials which resulted in membrane depolarization. More recent measurements of slow diffusion of K^+ between the t-tubule lumen and extracellular space led to the suggestion that similar changes of $[K^+]$ might occur within the t-tubule lumen (Swift et al. 2006). Such changes were not observed in our work: the small net K^+ flux across the t-tubule membrane resulted in mean $[K^+]_t$ remaining near $[K^+]_e$, even when the higher values of $\tau_{K,extt}$ from the work of Swift et al. (2006) were used. It is likely that the K^+ accumulation observed in frog ventricular muscle was because of slow K^+ diffusion from the extracellular clefts to the bulk solution ($\tau = 1$–5 s; DiFrancesco and Noble 1985); this is longer than the inter-stimulus interval and substantially slower than the rate of K^+ diffusion from t-tubules of isolated cells ($\tau_{K,extt} \sim 0.2$ s). When $\tau_{K,extt}$ was increased to 10 s in the model, we observed a cumulative increase of $[K^+]_t$ in response to a sudden increase of stimulation frequency (data not shown), comparable with that observed by Kline and Morad (1978) in extracellular clefts. The model also reproduced experimental results showing a transient increase in $[K^+]_t$ during a voltage-clamp pulse, as a result of K^+ flux into the t-tubular lumen via $I_{Kto,t}$ (Clark et al. 2001), and a marked $I_{K1,t}$ tail current because of the transient positive shift of K^+ reversal potential (Fig. 6). Modulation of $I_{K1,t}$, because of the decrease of $[K^+]_t$, was also observed during hyperpolarizing pulses in our former model (Pásek et al. 2003). Thus, although the model reveals transient changes in $[K^+]_t$, which might be further increased by local restriction of diffusion and/or heterogeneous K^+ channel distribution within the t-tubules, our work suggests that under steady-state conditions, without a restricted extracellular space, the small net K^+ flux across the t-tubule membrane causes only small deviations of mean $[K^+]_t$ from $[K^+]_e$.

Acknowledgments This work was supported by project MSM0021622402 from the Ministry of Education, Youth, and Sports of the Czech Republic, by project AV0Z 20760514 from the Institute of Thermomechanics of the Czech Academy of Science, and by the British Heart Foundation.

Appendix

See Tables 1, 2 and 3.

Table 1 Abbreviations used in the text

Symbol	Definition
LTCC	L-type Ca^{2+} channels
RyR	Ryanodine receptor
PKA	Protein kinase A
CDI	Ca^{2+}-dependent inactivation
VDI	Voltage-dependent inactivation
NSR	Network compartment of SR
JSR	Junctional compartment of SR
SR	Sarcoplasmic reticulum
AP	Action potential
VC	Voltage clamp
B_{htrpn}	Ca^{2+} buffer, high-affinity sites of troponin
B_{ltrpn}	Ca^{2+} buffer, low-affinity sites of troponin
B_{cm}	Ca^{2+} buffer, calmodulin
B_{cs}	Ca^{2+} buffer, calsequestrin
B_{ts}	Ca^{2+} buffer in t-tubular space
B_{ext}	Exogenous Ca^{2+} buffer

Table 2 Variables used in the text

Symbol	Definition
V_m	Membrane voltage
I_{Na}	Fast Na^+ current
I_{Ca}	L-type Ca^{2+} current
I_{Kto}	Transient outward K^+ current
I_{Kss}	Steady-state outward K^+ current
I_{K1}	Inward rectifying K^+ current
I_f	Hyperpolarization-activated current
I_{Kb}	Background K^+ current
I_{Nab}	Background Na^+ current
I_{Cab}	Background Ca^{2+} current
I_{NaCa}	Na^+–Ca^{2+} exchange current
I_{NaK}	Na^+–K^+ pump current
I_{pCa}	Ca^{2+} pump current
$I_{i,s}$	Surface membrane component of current i
$I_{i,t}$	Tubular membrane component of current i
J_{up}	Ca^{2+} flow via SR Ca^{2+} pump
$J_{x,net,t}$	Net flux of ion x through t-tubular membrane
$n_{x,net,t}$	Net amount of ion x transferred via t-tubules
$n_{x,net,t-e}$	Net amount of ion x diffusing from t-tubules to bulk extracellular space
$[x]_p$	Free concentration of substance x in the pipette
$[x]_e$	Free concentration of substance x in external space
$[x]_t$	Free concentration of substance x in t-tubular space
$[x]_c$	Free concentration of substance x in cytosolic space
$[x]_{st}$	Free concentration of substance x in t-tubular subsarcolemmal space
$[x]_{ss}$	Free concentration of substance x in surface subsarcolemmal space
$[x]_{dt}$	Free concentration of substance x in t-tubular dyadic space
$[x]_{ds}$	Free concentration of substance x in surface dyadic space
$[x]_{end}$	Free concentration of substance x at the end of cycle
$[x]_{peak}$	Maximum free concentration of substance x
$[x]_{mean}$	Mean free concentration of substance x
$[x]_{rest}$	Resting free concentration of substance x
$[Ca^{2+}]_{NSR}$	Free concentration of Ca^{2+} in NSR

Table 3 Parameters/constants used in the text

Symbol	Definition
V_t	Total volume of t-tubules
f	Stimulation frequency
F	Faraday constant
$\tau_{x,extt}$	Time constant of diffusion of ion x from external space to t-tubule lumen
$\tau_{pss,x}$	Time constant of diffusion of substance x from pipette to subsarcolemmal space
$\tau_{dsss,x}$	Time constant of diffusion of substance x from surface dyadic to subsarcolemmal space
$\tau_{dtst,x}$	Time constant of diffusion of substance x from t-tubular dyadic to subsarcolemmal space
$\tau_{ssc,x}$	Time constant of diffusion of substance x from surface subsarcolemmal to cytosolic space
$\tau_{stc,x}$	Time constant of diffusion of substance x from t-tubular subsarcolemmal to cytosolic space
$\tau_{ssst,x}$	Time constant of diffusion of substance x from surface to t-tubular subsarcolemmal space

References

Attwell D, Eisner D, Cohen I (1979) Voltage clamp and tracer flux data: effects of a restricted extra-cellular space. Q Rev Biophys 12:213–261

Baumgarten CM, Isenberg G, McDonald TF, Ten Eick RE (1977) Depletion and accumulation of potassium in the extracellular clefts of cardiac Purkinje fibers during voltage clamp hyperpolarization and depolarization: experiments in sodium-free bathing media. J Gen Physiol 70:149–169

Beuckelmann DJ, Wier WG (1988) Mechanism of release of calcium from sarcoplasmic reticulum of guinea-pig cardiac cells. J Physiol 405:233–255

Brette F, Rodriguez P, Komukai K, Colyer J, Orchard CH (2004a) β-adrenergic stimulation restores the Ca transient of ventricular myocytes lacking t-tubules. J Mol Cell Cardiol 36:265–275

Brette F, Sallé L, Orchard CH (2004b) Differential modulation of L-type Ca^{2+} current by SR Ca^{2+} release at the t-tubules and surface membrane of rat ventricular myocytes. Circ Res 95:e1–e7

Chase A, Orchard CH (2011) Ca efflux via the sarcolemmal Ca ATPase occurs only in the t-tubules of rat ventricular myocytes. J Mol Cell Cardiol 50:187–193

Chase A, Colyer J, Orchard CH (2010) Localised Ca channel phosphorylation modulates the distribution of L-type Ca current in cardiac myocytes. J Mol Cell Cardiol 49:121–131

Clark RB, Tremblay A, Melnyk P, Allen BG, Giles WR, Fiset C (2001) T-tubule localization of the inward-rectifier K^+ channel in mouse ventricular myocytes: a role in K^+ accumulation. J Physiol 537:979–992

DiFrancesco D, Noble D (1985) A model of cardiac electrical activity incorporating ionic pumps and concentration changes. Philos Trans R Soc Lond B Biol Sci 307:353–398

Eisner DA, Trafford AW, Díaz ME, Overend CL, O'Neill SC (1998) The control of Ca release from the cardiac sarcoplasmic reticulum: regulation versus autoregulation. Cardiovasc Res 38:589–604

Fabiato A (1985) Simulated calcium current can both cause calcium loading in and trigger calcium release from the sarcoplasmic reticulum of a skinned canine cardiac Purkinje cell. J Gen Physiol 85:291–320

Kline RP, Morad M (1978) Potassium efflux in heart muscle during activity: extracellular accumulation and its implications. J Physiol 280:537–558

Kohl P, Cooper PJ, Holloway H (2003) Effects of acute ventricular volume manipulation on in situ cardiomyocyte cell membrane configuration. Prog Biophys Mol Biol 82:221–227

McNary TG, Bridge JH, Sachse FB (2011) Strain transfer in ventricular cardiomyocytes to their transverse tubular system revealed by scanning confocal microscopy. Biophys J 100:L53–L55

Orchard CH, Pásek M, Brette F (2009) The role of mammalian cardiac t-tubules in excitation-contraction coupling: experimental and computational approaches. Exp Physiol 94:509–519

Pásek M, Christé G, Šimurda J (2003) A quantitative model of the cardiac ventricular cell incorporating the transverse-axial tubular system. Gen Physiol Biophys 22:355–368

Pásek M, Christé G, Šimurda J (2006) The functional role of cardiac t-tubules in a model of rat ventricular myocytes. Philos Trans R Soc A 364:1187–1206

Pásek M, Brette F, Nelson A, Pearce C, Qaiser A, Christé G, Orchard CH (2008) Quantification of t-tubule area and protein distribution in rat cardiac ventricular myocytes. Prog Biophys Mol Biol 96:244–257

Šimurda J, Pásek M, Christé G, Šimurdová M (2004) Modelling the distribution of $[Ca^{2+}]$ within the cardiac t-tubule—effects of Ca^{2+} current distribution and changes in extracellular $[Ca^{2+}]$ (Abstract). J Physiol 561P:PC5

Swift F, Strømme TA, Amundsen B, Sejersted OM, Sjaastad I (2006) Slow diffusion of K^+ in the T tubules of rat cardiomyocytes. J Appl Physiol 101:1170–1176

Trafford AW, Díaz ME, O'Neill SC, Eisner DA (1995) Comparison of subsarcolemmal and bulk calcium concentration during spontaneous calcium release in rat ventricular myocytes. J Physiol 488:577–586

Yao A, Spitzer KW, Ito N, Zaniboni M, Lorell BH, Barry WH (1997) The restriction of diffusion of cations at the external surface of cardiac myocytes varies between species. Cell Calcium 22:431–438